Supplementary information:

Controllable self-assembly of a novel Bi_2MoO_6-based hybrid photocatalyst: excellent photocatalytic activity under UV, Visible and Near-Infrared irradiation

Yuchen Hao, Xiaoli Dong*, Xiuying Wang, Shangru Zhai, Hongchao Ma and Xiufang Zhang

This SI file includes:

Detailed experimental methods

Figs. S1 to S12

Detailed experimental methods

Synthesis of nitrogen-doped carbon nanodots (NCDs)

The NCDs were successfully obtained by a simply solid-phase method. 300mg of Sodium Citrate anhydrous and 125mg urea were dispersed in 20mL of ultrapure water and ultrasound (200 W, 40 kHz) for 0.5 h. Then the mixture was stirring at 80 ^{o}C to collect the uniform mixture by dissolution-recrystallization. The 400mg as-prepared solid mixture was transferred into a Teflon-lined stainless steel autoclave, and heated at 180 ^{o}C for 1h. After cooled to room temperature, the final yellowish product was dispersed in 20 mL of ultrapure water and filtered through a 0.22um microporous membrane to remove the impurities and a yellow solution was separated. The final product solution was further dialyzed in a dialysis bag (retained molecular weight: 1000 Da), and light yellow solution of N-CQDs were obtained. After freeze drying, the products were dissolved in ethyl alcohol (1mg/mL) to further utilization and characterization.

Fabrication of NCDs/Bi-Bi_2MoO_6 (NCDs/Bi-BM) hybrid material

In a typical procedure, 0.6g Polyvinyl Pyrrolidone (PVP, K-30) were dissolved in 20 mL boiling ethylene glycol (EG) under magnetic stirring. After 4min later, 500mg $Bi(NO_3)_3·5H_2O$ and 121mg $Na_2MoO_4·2H_2O$ quickly dissolved in PVP solution within 10 min. After stirring for 30min and ultrasound for 1h, the mixture solution and 8mL NCDs solution (1mg/mL) were dropwised into 52ml ethanol, follow by stirring for 1h and ultrasound for 0.5h. The resulting solution was transferred into a 100 mL teflon-lined stainless steel autoclave, and heated to 170 ^{o}C for 24h. After the autoclave was air-cooled to room temperature, the mixture was centrifugaled, washed with distilled water and ethyl alcohol. After freeze drying for 48h, the NCDs/Bi-Bi_2MoO_6 (NCDs/Bi-BM) hybrid material was obtained. On the other hand, the Bi-Bi_2MoO_6 (Bi-BM) hybrid material was synthesized by the same method but without NCDs to add. Moreover, the optimal loading level was investigated by the photodegradation experiments with different samples as photocatalyst (Fig. S1).

Fabrication of conventional Bi_2MoO_6 (C-BM) hollow

The conventional Bi_2MoO_6 hollow was prepared by traditional hydrothermal method. In a typical procedure, 242mg $Bi(NO_3)_3 \cdot 5H_2O$ and 58mg $Na_2MoO_4 \cdot 2H_2O$ were dissolved in 10 mL of ethylene glycol (EG) respectively under magnetic stirring. After completely dissolved, the two solutions were mixed together, then the mixture solution were dropwised into 30ml ethanol, follow by stirring for 20 min, and the resulting solution was transferred into a 50 mL Teflon stainless steel autoclave, and heated to 160 ^oC for 20h. After the autoclave was air-cooled to room temperature, the mixture was centrifugaled, washed with distilled water and ethanol, and dried at 80 C in air.

Characterization.

The crystallinity and the purity of the as-prepared samples were characterized by powder X-ray diffraction (XRD) analysis on a Shimadzu XRD-6100 diffractometer at 40 kV and 40 mA with Cu Ka radiation. Data were recorded at a scan rate of 0.1^o/s in the 2θ range 10^o-70°. X-ray photoelectron spectroscopy (XPS) measurement by a Thermo VG ESCALAB-250 system with Al-K and Mg-K source operated at 15kV. The N_2-sorption measurement was performed by using Micromeritics Tristar3000 at 77K, the specific surface area and the poresizedistribution were estimated using the BET and BJH methods, respectively. The TEM analyses were performed by a JEOL JEM-2100F transmission electron microscope. SEM images were taken using a field-emission scanning electron microscope (JSM-7800F, JEOL). Light absorption property was evaluated by UV-Vis diffuse reflectance spectra (UV-vis DRS, CARY 100&300, VARIAN), $BaSO_4$ was used as a reflectance standard. The PL spectra of the photocatalysts were analysed using a Hitachi F-7000 fluorescence spectrophotometer.

Photoelectrochemical test

Photoelectrochemical measurements were performed on CHI660E electrochemical workstation (Shanghai Chenhua, China) using a three-electrode configuration and the as-prepared samples as working electrode. The working electrodes were prepared by dip-coating method, 4 mg of sample was suspended in 4mL of DMF to produce slurry, which was then dip-coated onto a glass carbon electrode and all the investigated electrodes show a similar thickness. The light source is a 300 W Xe lamp. A mixture of 0.1 M Na_2SO_4 (fisher) in deionized water (PH=7) aqueous solution was used as the electrolyte in the experiments. Electrochemical impedance spectroscopy (EIS) was conducted using CHI660E with an alternating current signal (10mV) in the frequency range of 0.1-10^5Hz at open circuit potential (OCP). Mott-Schottky plots were measured at a frequency of 100 kHz in the dark. The J-V curve of the working electrode was obtained by the linear sweep voltammogram (LSV) with a scan rate of 10 mV/s. In some experiments, band pass filters (400nm, 520nm) and 780nm cut filter were used to decouple the different stages of photoreaction under different wavelengths light irradiation.

Photocatalytic activity measurements

The light source for photocatalytic reaction was a 300 W Xe lamp (PLS-SXE 300, Beijing Perfect Light Co., Ltd.). And the photocatalytic activity of the as-prepared catalysts under simulated sunlight was estimated by measuring the degradation rate of RhB, BPA (10 mg/L) and photoreduction rate of Cr(VI) (10 mg/L, based on Cr(VI) in a dilute $K_2Cr_2O_7$ solution) in an aqueous solution. 10mg photocatalyst were added in quartz reactor which contained 50mL aqueous solution. In the process of degradation, a certain volume of suspension was sampled every 10 min, then centrifuged immediately to remove the catalysts. The absorbance was measured by UV-vis spectrophotometer and the normalized concentration changes of RhB, BPA and Cr(VI) (C/C_0) were obtained based on the maximum absorption at 554 nm, 278 nm and 371 nm. The reusability and stability of the photocatalysts was measured via repeating the uniform experiment for four more times.

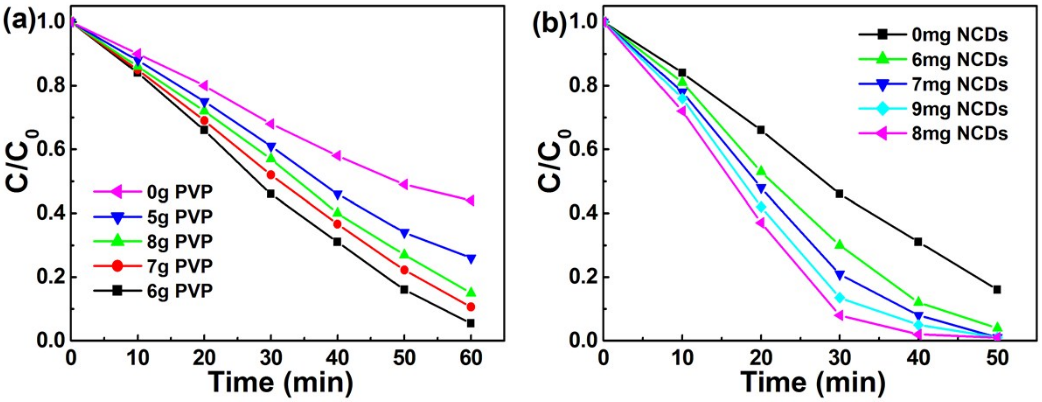

Fig. S1 Photocatalytic degradation of RhB in the presence of different photocatalyst with different weight ratios PVP (only Bi-BM, no NCDs deposition) (a) and GQDs (b) under artificial solar light irradiation.

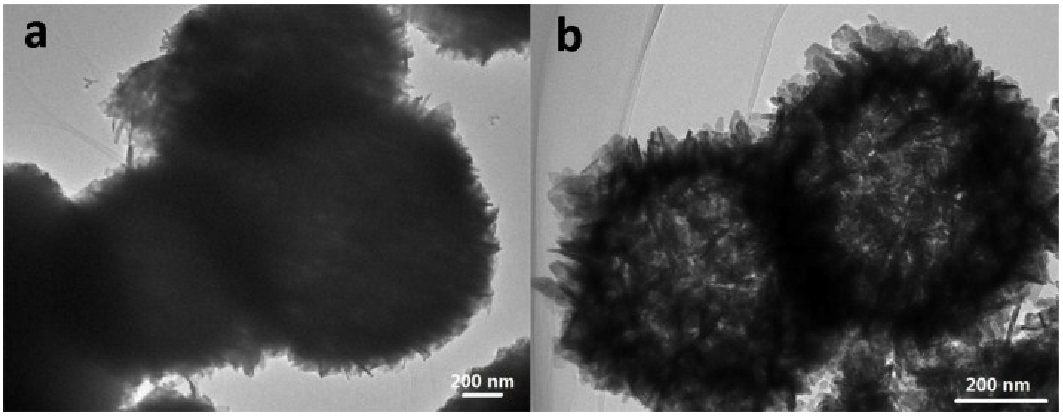

Fig. S2 TEM images of conventional Bi_2MoO_6 hollow (a) and ultrathin NCDs/Bi-BM hollow (b).

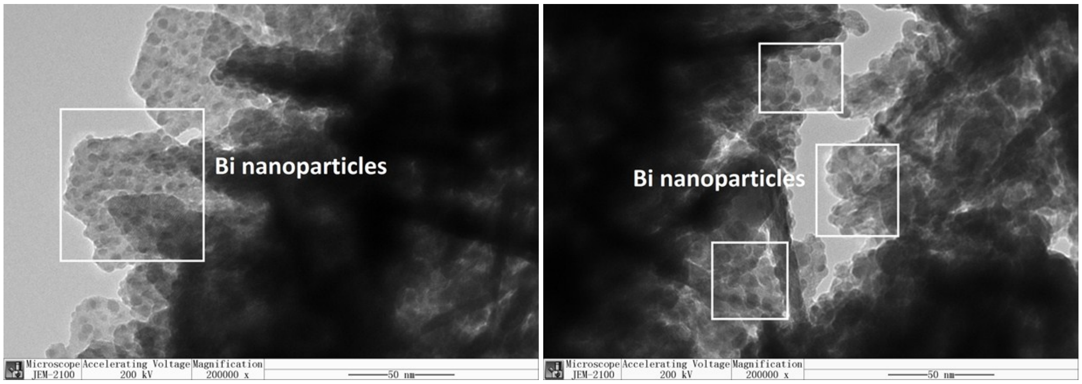

Fig. S3 TEM images of ultrathin NCDs/Bi-BM nanohollow.

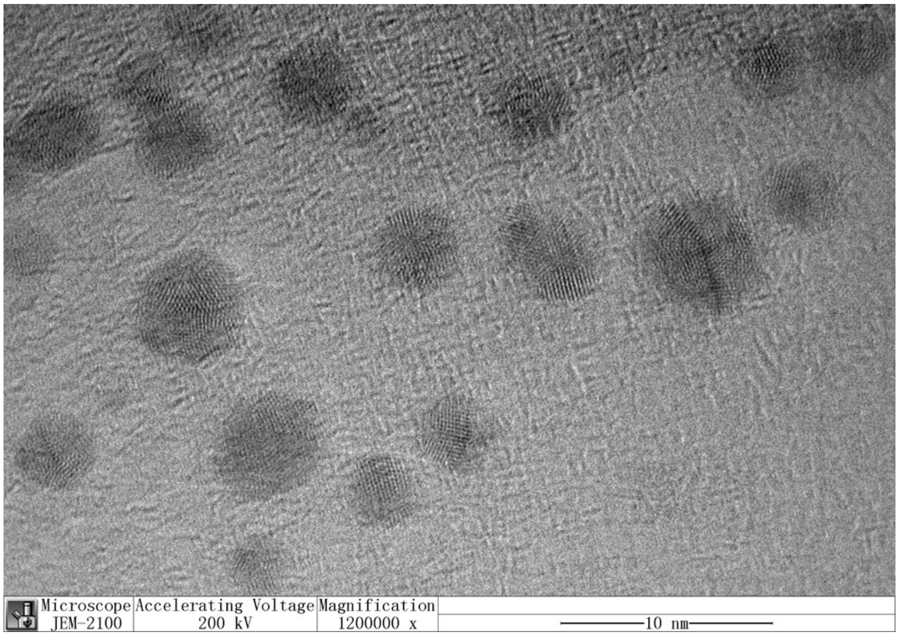

Fig. S4 TEM images of the as-prepared nitrogen-doped carbon nanodots (NCDs).

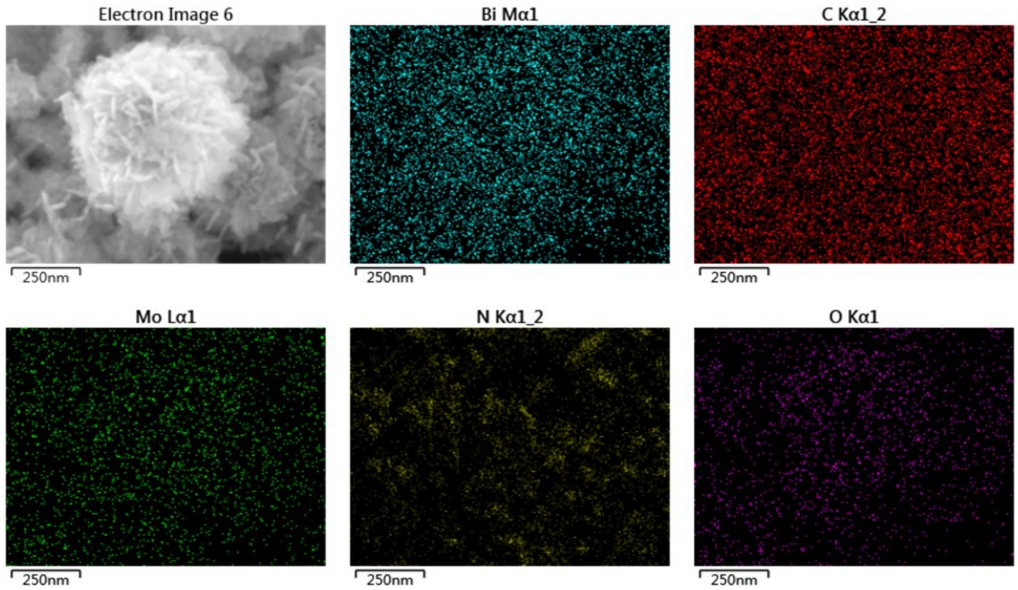

Fig. S5 FESEM image and corresponding elemental mappings of the NCDs/Bi-BM hybrid.

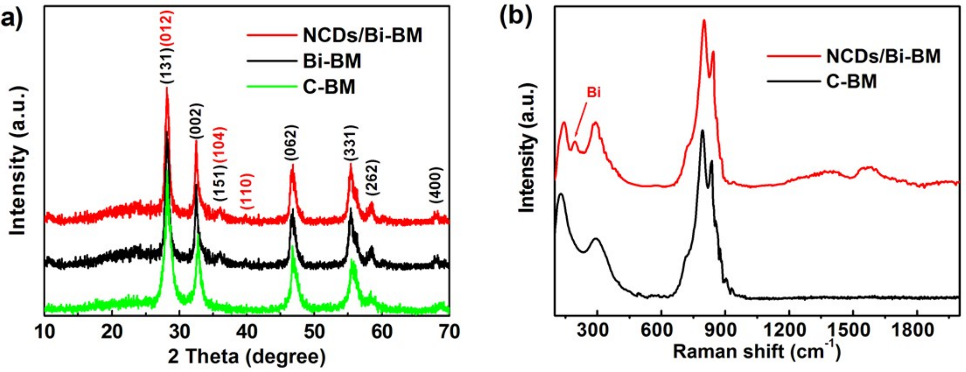

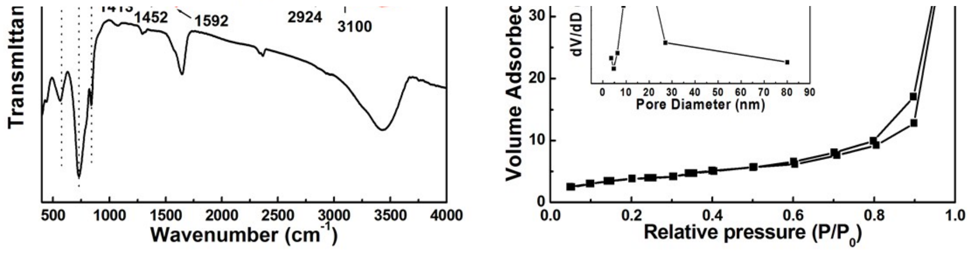

Fig. S6 (a) XRD patterns of as-prepared NCDs/Bi-BM, Bi-BM and C-BM. (b) Raman spectrum, (c) FT-IR spectrum of NCDs/Bi-BM and C-BM. (d) Nitrogen adsorption-desorption isotherm and pore size distributions (inset) of NCDs/Bi-BM hybrid. Note that the Raman spectra of NCDs/Bi-BM were obtained by deducting the background of NCDs owing to its strong photoluminescence effect during characterization.

The XRD patterns of as-prepared C-BM, Bi-BM and NCDs/Bi-BM were shown in Fig. S5a, the distinct diffraction peaks at 2θ of 28.3°, 32.8°, 47.1°, 55.4°, 58.5°, and 68.2° corresponding to (131), (002), (062), (331), (262) and (400) crystal planes of orthorhombic Bi_2MoO_6 (JCPDS no.84-0787), and there are no other impurity phase, indicating the high purity of the Bi_2MoO_6 as prepared. For the Bi-BM hybrid, the peaks at 36°, and 39.8° corresponding to (104) and (110) crystal planes of Bi metal. For the NCDs/Bi-BM nanocomposite, no observation diffraction peak from NCDs due to the relatively limited NCDs amount in the NQDs/Bi-BM hybrid material. Fig. S5b shows the Raman spectrum of C-BM and NCDs/Bi-BM, the distinct peaks at 294, 808 and 844 cm^{-1} for pure Bi_2MoO_6 which has been reported[1]. The two special Raman peaks at 1370 cm^{-1} (D band) and 1580 cm^{-1} (G band) are also observed in Raman spectra of NCDs/Bi-BM hybrid which can be attributed to graphite carbon and amorphous carbon, respectively. Moreover, the obvious peak at 197 cm^{-1} belongs to the Bi metal. To further ensure the presence of NCDs in NCDs/Bi-BM hybrid material, FT-IR spectra was carried out and the interaction between NCDs and Bi_2MoO_6 can be further investigated. From Fig. S5c, both C-BM and NCDs/Bi-BM nanocomposite can be found a series of peaks in the FT-IR spectra. The absorption bands at 842 cm^{-1} be identified based on asymmetric and symmetric vibration modes (Mo-O stretching) of the corner sharing $(MoO_6)^{6-}$ octahedron, while the peaks located at 567 and 734 cm^{-1} was assigned as the asymmetric stretching mode and the bending vibration of the MoO_6 which can prove existence of pure Bi_2MoO_6. But for NCDs/Bi-BM hybrid material, the peaks at 1413 cm^{-1} and 1452 cm^{-1} are deemed to the typical stretching modes of CN heterocycles, proving the triazine units remain in the NCDs. The peak around 3100 cm^{-1} is considered to N-H stretching. Moreover, the strong peak at 1592 cm^{-1} can be considered to the stretching vibrations of carboxylate anions in the hydrophilic carboxylate groups which are belong to the NCDs. From above conclusion, we can further confirm that the NCDs and Bi metal were successfully deposited on the ultrathin Bi_2MoO_6 nanohollow. The N_2 adsorption-desorption isotherms (Fig. S5d) and pore size distributions (inner Fig. S5d) can be used to determine the surface area and pore types of the NCDs/Bi-BM hybrid. The as prepared sample with type IV classification and H3 type hysteresis, which indicate that the as-prepared NCDs/Bi-BM hybrid with a mesoporous structure.

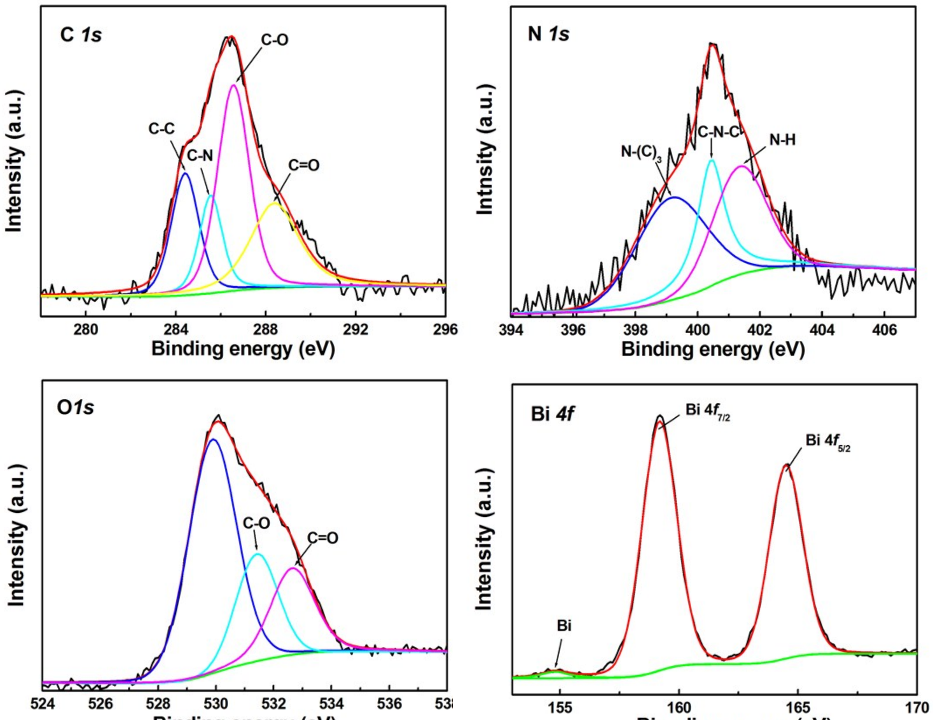
C 1s
C-C
C-N
C-O
C=O
Intensity (a.u.)
280
284
288
292
296
Binding energy (eV)
N 1s
N-(C)$_3$
C-N-C
N-H
Intnsity (a.u.)
394
396
398
400
402
404
406
Binding energy (eV)
O1s
C-O
C=O
Intensity (a.u.)
524
526
528
530
532
534
536
Bi 4f
Bi 4f$_{7/2}$
Bi 4f$_{5/2}$
Bi
Intensity (a.u.)
155
160
165
170

Fig. S7 High-resolution C 1s, N 1s, Bi 4f and O 1s XPS spectra of NCDs/Bi-BM hybrid material.

The XPS analysis shown in Fig. S6 was performed to understand the chemical composition of C, N, Bi and O in NCDs/Bi-BM nanocomposite. From the high-resolution C1s spectrum, the peaks at 284.3 eV and 285.5 eV reflect the C-C coordination and the bonding structure of C-N bonds, the other two peaks at 286.5 eV and 288.4 eV are attributed the C-O and C=O bonds, respectively. For the N1s high-resolution spectrum, the peaks located at 400.4 eV, 399.2 eV and 401.4 eV corresponds to C-N-C, N-$(C)_3$ and N-H groups, respectively. The high-resolution Bi 4f spectrum with obvious peak at 159.1 eV ($Bi4f_{7/2}$) and 164.5 eV ($Bi4f_{5/2}$), are ascribed to Bi^{3+}. Additionally, the weaker peak around 154.7 eV belongs to Bi metal. The high-resolution O1s spectrum shows three different peaks at 530 eV, 531.5 eV, 532.8 eV belongs the lattice oxygen of Bi_2MoO_6, C-O and C=O from NCDs, respectively.

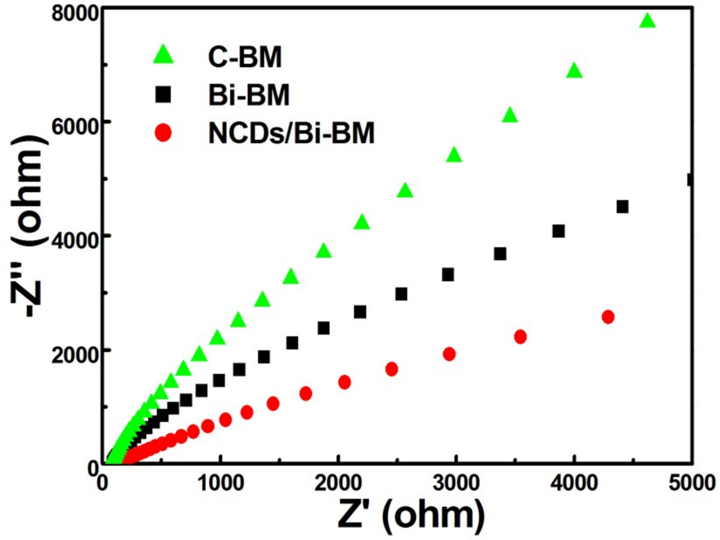

Fig. S8 EIS Nyquist plots of C-BM, Bi-BM and NCDs/Bi-BM hybrid.

Fig. S9 Color evolution of the series of different samples

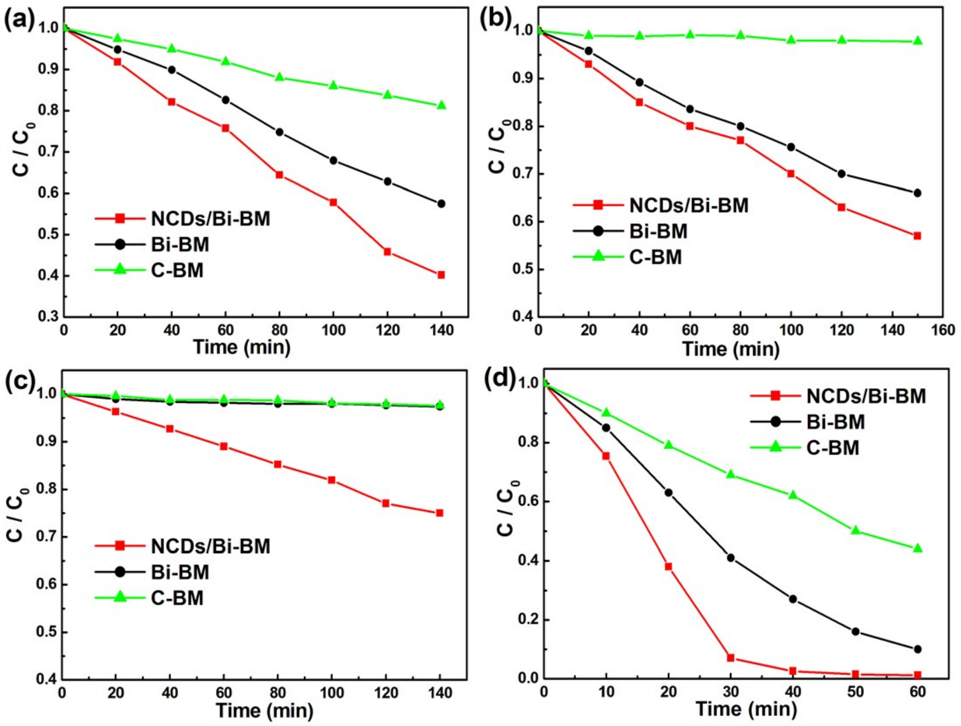

Fig. S10 Photocatalytic degradation curves of C-BM, Bi-BM and NCDs/Bi-BM under 420 nm monochromatic light (a), 520 nm monochromatic light (b), NIR light (c) and simulated sunlight (d) irradiation.

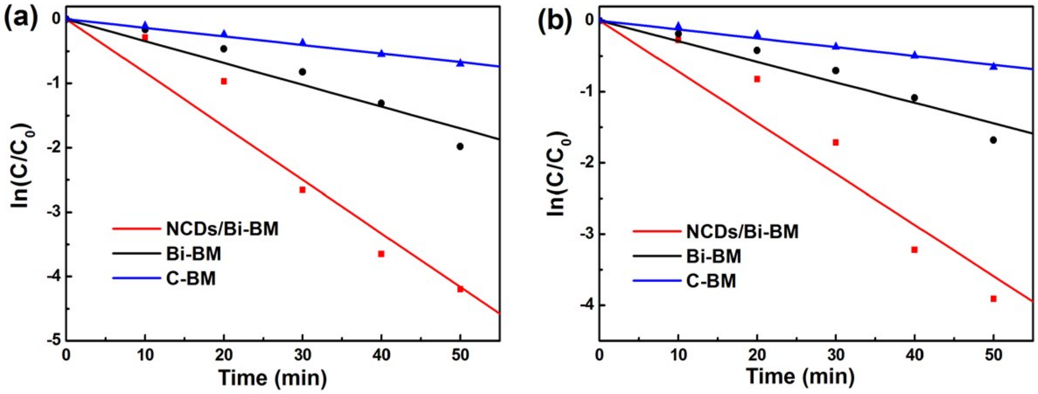

Fig. S11 Linear transform $\ln(C/C_0) = f(t)$ of the kinetic curves of BPA degradation (a) and Cr(VI) reduction (b).

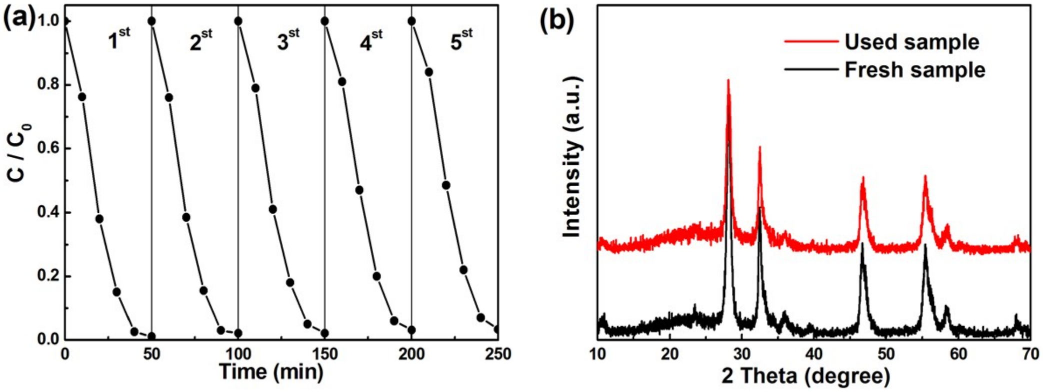

Fig. S12 (a) Recycling runs of the NCDs/Bi-BM hybrid under simulated sunlight irradiation, (b) XRD patterns of NCDs/Bi-BM before and after photo-degradation of RhB.

The reusability and stability of photocatalysts are very important to the practical application. To evaluate the reusability and stability of NCDs/Bi-BM hybrid material, recycling experiment are performed for the decomposition of RhB under simulated sunlight irradiation (Fig. S10a). After five cycles, the photoreactivity of NCDs/Bi-BM not found significant decrease, indicating this hybrid material with high stability. The XRD spectrum of NCDs/Bi-BM hybrid material before and after the photocatalytic reactions are shown in Fig. S10b, the crystal structures of the NCDs/Bi-BM nanocomposite is no obvious change, which further ensure the stability of NCDs/Bi-BM hybrid material.